World Scientific Research Journal Volume 9 Issue 5, 2023
ISSN: 2472-3703 DOI: 10.6911/WSRJ.202305_9(5).0013

Finite Element Analysis of Axial Compression Performance of Concrete Filled Square Steel Tubular Columns with Void Defects

Tianyu Shang

College of Civil Engineering, Henan Polytechnic University, Jiaozuo, 454000, China

Abstract

In order to study the influence of void defects on the axial compression performance of concrete-filled square steel tubular columns, the axial compression model of concrete-filled square steel tubular columns with void defects was established by ABAQUS software with the density loss rate of core concrete, the number of void edges and the position of void as the main parameters. The calculation results show that when the density loss rate of core concrete is 1 %, the influence of void positions on both sides on the specimens is almost the same. The ultimate bearing capacity and deformation capacity of the specimens decrease significantly with the increase of the number of void edges.

Keywords

Square steel tube concrete column; Axial compression; Void defect.

1. INTRODUCTION

The traditional concrete structure needs to be supported in advance before pouring, and the steel bars need to be tied up. After the concrete is condensed, the formwork needs to be removed, which reduces the construction efficiency. The concrete filled steel tube column effectively improves the above shortcomings, and the material performance can be fully utilized. The simple construction method reduces the construction period, improves the construction efficiency, and saves the construction cost[1]. With the deepening of the research on the mechanical properties of concrete filled steel tube and the innovation of construction technology, square concrete filled steel tube columns are widely used in high-rise and super high-rise buildings, long-span arch bridges and underground engineering[2-3].

However, the concrete pouring in the steel tube cannot directly observe the pouring quality. Errors often occur in the construction process of such concealed projects, resulting in void defects inside the steel tube. The main reasons for the void defects are as follows : (1) The hardening and shrinkage of the core concrete leads to a gap between the core concrete and the steel tube wall, forming a void defect ; (2) If there is no rust removal or incomplete rust removal in the steel tube wall, the concrete in these parts is difficult to bond with the steel tube, which is easy to cause void. (3) The difference of expansion coefficient between concrete and steel tube and the temperature difference lead to the separation of concrete and steel tube wall.

At present, relevant scholars have carried out research on the mechanical properties of concrete-filled steel tubular columns with void defects, and have obtained some useful conclusions. Han[4-5] et al.carried out axial compression and eccentric compression tests on 12 concrete-filled steel tubes with void defects. The main parameters were : circumferential void and spherical crown void. Based on the test, a finite element model was established. The simulation results were consistent with the test results. The influence of different parameters on the ultimate strength of concrete filled steel tubular columns with void defects is revealed.

ISSN: 2472-3703 DOI: 10.6911/WSRJ.202305_9(5).0013

Lu[6-7] et al.carried out axial compression and eccentric compression tests on concrete-filled steel tubular members with composite defects. The main parameters were void ratio and porosity. Based on the test, a finite element model was established and consistent with the test results. The test results show that the bearing capacity of concrete filled steel tubular members decreases with the increase of porosity of core concrete. Reducing the void ratio and porosity of arch bridge is the key to ensure the reliability of concrete filled steel tube. The finite element model of Liao, Han, Tao et al.underestimates the loss of ultimate bearing capacity of CFST columns caused by void ratio. With void ratio, concrete strength and steel tube strength grade as the main variable parameters, Wang[8] completed the axial compression test of 12 elliptical section concrete filled steel tubes, and established the model by finite element software. The results show that the void defect causes brittle cracking of the core concrete, and the local deformation of the concrete filled steel tubular column is serious. The void ratio is between 0.7 % and 6.5 %, the bearing capacity of the specimen is reduced by 18.5 % -34.5 %, the initial stiffness is reduced by 5.4 % -17.8 %, and the ductility is reduced by 17.0-31.4 %. The void defect weakens the restraint effect of steel tube on concrete. With the increase of strength grade of concrete and steel tube, the influence of void defect can be effectively weakened.

In summary, domestic and foreign scholars ' research on void mainly focuses on concrete-filled circular steel tubular columns, and there are few studies on concrete-filled square steel tubular columns with void defects, and the concrete strength grade is low ; the void defect is considered single, only considering the void rate and void height ; based on this, this paper analyzes the void defect from the macro perspective of the loss rate of the compactness of the core concrete. Under the analysis of the loss rate of the compactness of the core concrete is 1 %, the void position and the number of void edges are the main change parameters. The ABAQUS finite element software is used to establish the axial compression model of the void defect of the concrete filled square steel tubular column. At the same time, the axial compression test of five concrete filled square steel tubular columns (including void defects) of our research group is cited. The calculated values are compared with the measured values, and the accuracy of the finite element model is verified. The failure mode, load-displacement / strain curve, bearing capacity and energy dissipation capacity of concrete-filled square steel tubular columns with void defects under the above parameters are studied and analyzed.

2. TEST OVERVIEW

In this paper, a total of 5 concrete-filled square steel tubular columns were designed, 1 was a defect-free comparison specimen and 4 specimens with void defects. The detailed parameters of the specimens are shown in Table 1. The specimens with void defects include bilateral voids on the opposite side, bilateral voids on the adjacent side, three-sided voids and four-sided voids. The void schematic diagram is shown in Figure 1.

Table 1. Void defect specimen parameters

Specimen name	Steel pipe size $B \times t$ / mm /	concrete strength f_{cu} / MPa	specimen height H / mm	defect type	Density loss rate ρ_l / %	Number of empty edges
CFST-M	200/3.75	C60	600	zero defect	0	0
CFSTE-1	200/3.75	C60	600	Opposite side void	1	2
CFSTE-2	200/3.75	C60	600	Adjacent side void	1	2
CFSTE-3	200/3.75	C60	600	Trilateral void	1	3
CFSTE-4	200/3.75	C60	600	Four sides void	1	4

ISSN: 2472-3703 DOI: 10.6911/WSRJ.202305_9(5).0013

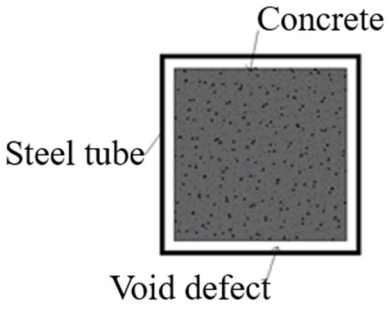

Figure 1. Void defect diagram

3. FINITE ELEMENT MODEL ESTABLISHMENT AND VERIFICATION

In this paper, Q355b low carbon steel is often used in building structure. The stress-strain curve is divided into elastic section, elastic-plastic section, plastic section, strengthening section and secondary plastic flow stage. The specific relationship between stress and strain is shown in Formula 1.

$$\sigma=\begin{cases} E_S\varepsilon & (\varepsilon\le\varepsilon_e) \\ f_p+\dfrac{\varepsilon-\varepsilon_e}{\varepsilon_{e1}-\varepsilon_e}(f_y-f_p) & (\varepsilon_e<\varepsilon\le\varepsilon_{e1}) \\ f_y & (\varepsilon_{e1}<\varepsilon\le\varepsilon_{e2}) \\ f_y+\dfrac{\varepsilon-\varepsilon_{e2}}{\varepsilon_{e2}-\varepsilon_{e1}}(f_u-f_y) & (\varepsilon_{e2}<\varepsilon\le\varepsilon_{e3}) \\ f_u & (\varepsilon>\varepsilon_{e3}) \end{cases} \tag{1}$$

Of which:

$$\varepsilon_e=\frac{0.8f_y}{E_S} \qquad \varepsilon_{e1}=1.5\varepsilon_e \qquad \varepsilon_{e2}=10\varepsilon_{e1}\varepsilon_{e3}=100\varepsilon_{e1} \tag{2}$$

In the formula : E_S is the elastic modulus of steel, f_p is the proportional limit of steel， f_y is the yield strength of steel， f_u is the tensile strength limit of steel， ε_e the elastic strain end point of material, ε_{e1} the elastic-plastic strain end point of material, ε_{e2} the plastic end position, ε_{e3} tensile strength strain.

The concrete adopts the CDP plastic damage constitutive model. Considering the restraint effect of steel tube on concrete, the stress-strain curve suitable for concrete filled steel tube proposed by Han Linhai is selected.

$$y=\begin{cases} 2x-x^2 & x\le 1 \\ \dfrac{x}{\beta_0(x-1)^\eta+x} & x>1 \end{cases} \tag{3}$$

Among them:

$$x=\frac{\varepsilon}{\varepsilon_0} \qquad y=\frac{\sigma}{\sigma_0} \tag{4}$$

$$\sigma_0=f_c^{'} \qquad \varepsilon_0=\varepsilon_c+800\xi^{0.2}\times10^{16} \qquad \varepsilon_c=(1300+12.5\times f_c^{'})\times10^{16} \tag{5}$$

ISSN: 2472-3703 DOI: 10.6911/WSRJ.202305_9(5).0013

$$\eta = 1.6 + \frac{1.5}{x} \qquad \beta_0 = \frac{\left(f_c^{'}\right)^{0.1}}{1.2(1+\xi)^{0.5}} \qquad \xi = \frac{A_S \times F_S}{A_C \times F_C} \tag{6}$$

In the formula : ξ Effective constraint effect coefficient, $f_c^{'}$ For cylinder concrete compressive strength. β_0 It is a constraint effect related variable. σ_0 The peak stress. ε_0 The peak strain. ε_c It is the peak strain of unconstrained concrete. η is the parameter of the descending segment.

3.1. Create parts and material properties

The geometric shape of the component is defined in the Part module of the finite element software, and each component of the analysis model is created. The components of the specimen are shown in Figure 2. According to the above constitutive formula, the stress and strain data obtained by solving different materials are input according to the corresponding material model, and the cross section is created and given to the three-dimensional entity.

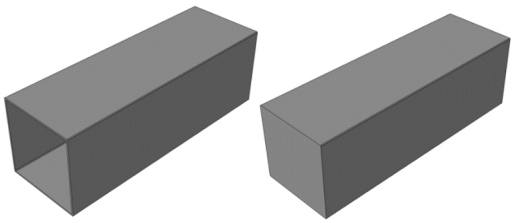

(a) steel tube (b) core concrete

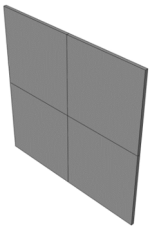

(c) steel plate

Figure 2. Parts of a typical specimen

3.2. Assembly parts

After the creation of the two components of the steel pipe and the core concrete, because they exist independently in their respective local coordinate systems, in order to form a complete assembly, the two components need to be positioned and assembled in the overall coordinate system, Figure 3 is the overall assembly diagram of the components.

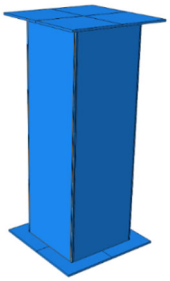

Figure 3. Assembly example

ISSN: 2472-3703 DOI: 10.6911/WSRJ.202305_9(5).0013

3.3. Coupling constraints

Referring to the actual loading and constraint conditions in the axial compression test of concrete-filled square steel tubular columns, a reference point is set at the center of the steel plates at the upper and lower ends of the specimen respectively. In order to effectively control the same displacement of the upper surface of the model during the whole loading process, the reference point and the upper compression surface of the model are coupled and constrained, and the load is applied at the reference point to fully ensure that the end of the model is uniformly compressed. The established coupling constraint model is shown in Figure 4.

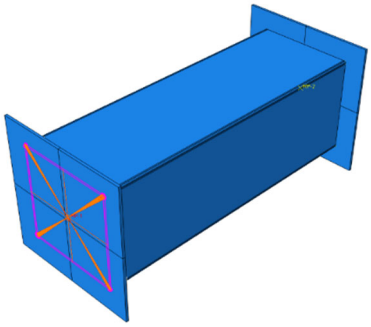

Figure 4. Coupling constraints

3.4. Contact relationship between steel tube and concrete

ABAQUS software provides a variety of contact relationships[9]. The interface properties of steel tube and concrete are more complex. In view of the difference between core concrete and steel tube in the axial compression test of square steel tube concrete column, there is a limited sliding phenomenon between steel tube and core concrete. Therefore, the friction type contact relationship is adopted, and the friction coefficient of 0.6 is used instead of the bond slip force according to the test summary of a large number of steel tube concrete by Han Linhai, which is conducive to calculation convergence. The established contact relationship model is shown in Figure 5.

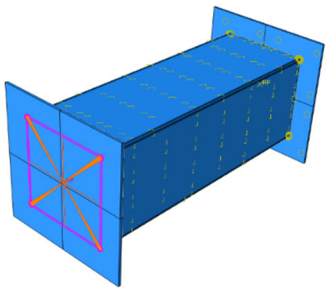

Figure 5. Contact constraint

3.5. Determine the boundary conditions

In the interaction module, the upper and lower plates are coupled with a reference point at their center respectively. In the boundary condition part, the degree of freedom of the reference point of the lower plate is fixed, and the upper plate will be constrained by the translational degree of freedom. The loading method adopts displacement control, and Figure 6 is the boundary condition diagram.

ISSN: 2472-3703 DOI: 10.6911/WSRJ.202305_9(5).0013

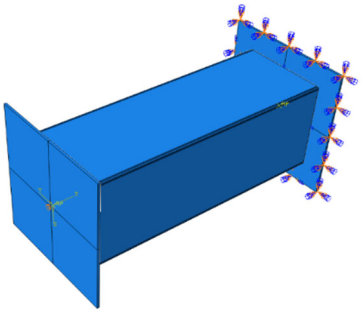

Figure 6. Boundary conditions

3.6. Unit selection

In order to increase the calculation accuracy of the model simulation, combined with the actual properties of the test materials, the three-dimensional solid element C3D8R is used for the steel tube, and the rigid element S4R is used for the upper and lower steel plates. Considering that the model calculation of the solid element C3D20 and the element entity C3D8R is similar, so in order to facilitate the calculation and reduce the calculation time, the core concrete in this paper also uses the three-dimensional solid element C3D8R.

3.7. Meshing

Free grid, structured grid and swept grid are three commonly used grid division techniques in ABAQUS software[10].In this paper, the model steel tube and core concrete adopt structured grid division technology. When the model is meshed, the mesh size is appropriately reduced at the stress concentration of the model and the part where the stress and strain need to be observed, and the mesh size is appropriately enlarged at the part where the model does not need too much observation. This not only accelerates the calculation speed of the software but also ensures the calculation accuracy, while taking into account the convergence of the model.

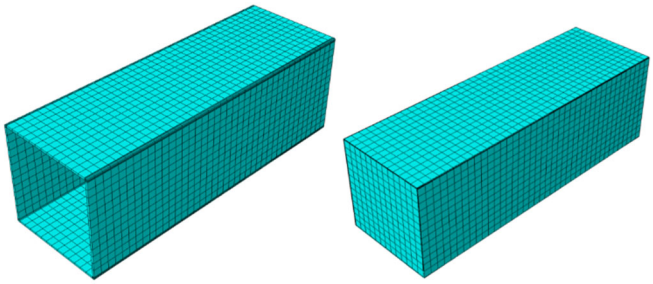

(a) square steel tube (b) Defect-free core concrete

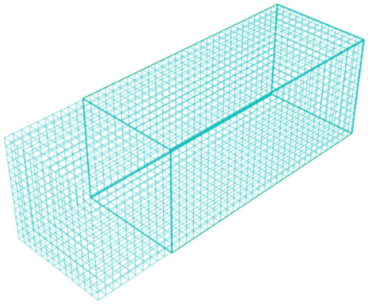

(C) Void defect core concrete

Figure 7. Schematic diagram of the mesh of the model and parts

ISSN: 2472-3703 DOI: 10.6911/WSRJ.202305_9(5).0013

4. VERIFICATION OF FINITE ELEMENT ANALYSIS RESULTS OF SQUARE CONCRETE FILLED STEEL TUBULAR COLUMN

Due to the limited space, the failure characteristics and load-displacement curves of CFST-W and CFSTE-4 were compared with the finite element simulation results.

4.1. Failure modes

(1) No defect specimen

The failure characteristics of CFST-W are compared with the MISES stress cloud diagram simulated by ABAQUS. The stress-strain nephogram of the peak point of CFST-W steel tube and core concrete is shown in Figure 8.

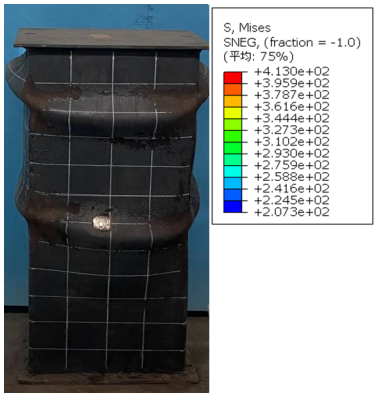

(a) The failure mode of CFST-M specimen

(b) Mises stress cloud of steel pipe

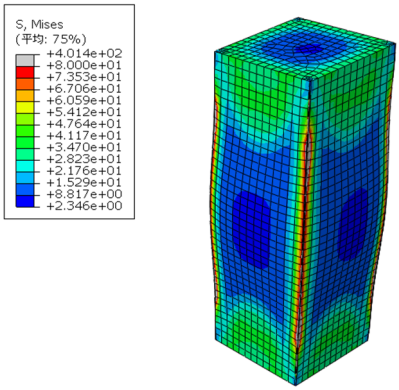

(c) Mises stress nephogram of core concrete

Figure 8. Mises stress cloud for defect-free model (CFST-W)

It can be seen from Figure 8 that when the load increases to the peak bearing capacity, the stress in the middle of the CFST-W specimen is large, and a ring of buckling is formed in the middle. The stress at the upper and lower ends of the core concrete is large, and the stress in the middle, upper and lower ends of the steel tube and the corner is large. The failure mode of the defect-free model is the classical buckling failure in the middle, which is basically consistent with the experimental failure mode. The rationality of the constitutive relationship and contact relationship of each material selected by the model is verified, which shows the feasibility of using ADAQUS to simulate and analyze the axial compression performance of square concrete-filled steel tubular columns.

(2) Void defect

ISSN: 2472-3703 DOI: 10.6911/WSRJ.202305_9(5).0013

The failure characteristics of CFSTE-4 with four-sided void defects were compared with the MISES stress cloud diagram simulated by ABAQUS. The stress-strain cloud diagram of the peak point of CFSTE-4 steel tube and core concrete is shown in Fig.9.

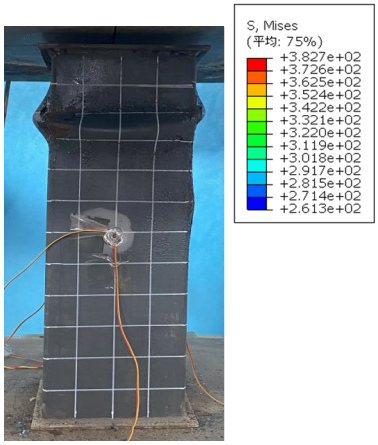

(a) Failure mode of CFSTE-4

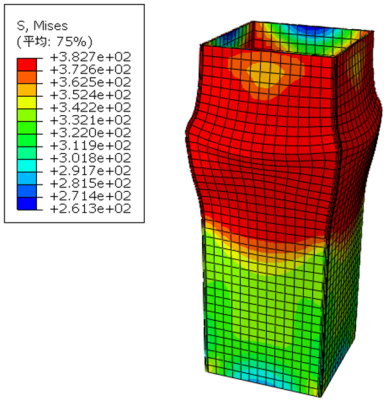

(b) Mises stress cloud of steel pipe

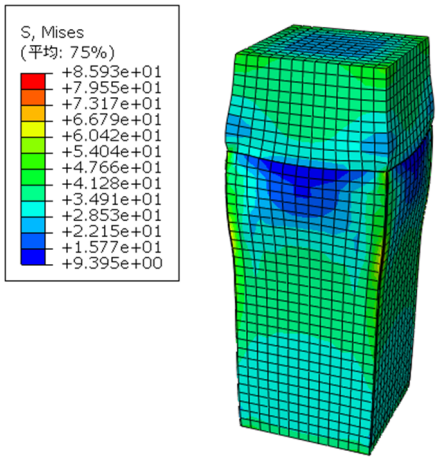

(c) Mises stress nephogram of core concrete

Figure 9. Mises stress cloud of the debonding defect model

From Figure 9, it can be seen that the model has a banded area with large stress at the place where the void defect is generated and in the middle. The steel tube wall has a local bulge at the place where the void defect is generated. The upper part of the four-sided void defect specimen has a more serious local buckling. When loading to the peak bearing capacity, the strain development of the void model and each component is mainly concentrated near the void defect. This phenomenon is similar to the failure characteristics observed in the loading of the specimen. During the loading process of the specimen, when the CFSTE-4 specimen is loaded to the peak load, the bulge of the steel tube wall near the defect of the specimen develops into a circle of bulging.

4.2. Load-displacement curve

Taking CFST-W and CFSTE-4 as examples, the calculated results of ABAQUS model and the measured load-displacement curves are shown in Figure 8:

ISSN: 2472-3703 DOI: 10.6911/WSRJ.202305_9(5).0013

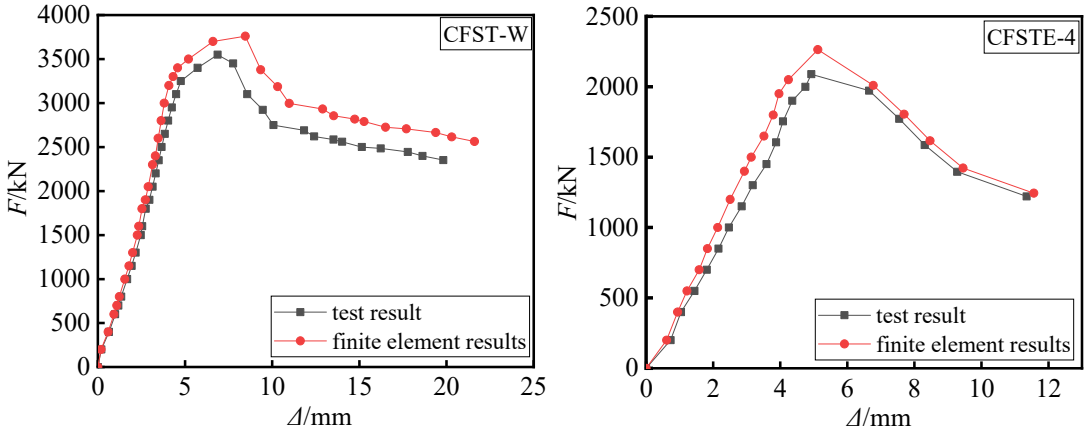

Figure 10. Comparison of calculated results of model and measured load-displacement curve

Comparing the calculation results of ABAQUS software with the test results of the same research group, it can be seen that the error of the ultimate bearing capacity of the specimens is within 10 %, and the load-displacement curve drawn by the finite element simulation results is similar to the test results. The load-displacement curve of the model shows a linear rise stage, a slow rise stage with defects, and a decline stage after the peak load. At the initial stage of loading, the internal defects of core concrete have little effect on the specimen, and the load-displacement curve of the model increases linearly. With the increase of load, the concrete near the defects is gradually crushed, the lateral deformation coefficient of core concrete increases gradually, and the slope of the load-displacement curve of the model decreases gradually. After the peak load, due to the defects contained in the core concrete, the descending section of the load-displacement curve of the model is different. The descending section of the load-displacement curve of the square concrete filled steel tube without defects is relatively slow, indicating that the specimen has good deformation ability, but when the square concrete filled steel tube column has four-sided voids. The descending section of the load-displacement curve of the specimen is steep, indicating that the failure stage of the specimen is relatively short and the deformation ability of the specimen is poor.

4.3. Analysis and comparison of bearing capacity

Table 2 is the comparison between the finite element analysis results and the measured bearing capacity.

Table 2. Comparison of finite element analysis results and measured bearing capacity

Specimen name	defect type	Density loss rate /%	Measured bearing capacity /kN	Simulated bearing capacity /kN
CFST-M	zero defect	0	3550	3760
CFSTE-1	Opposite side void	1	2799	2865
CFSTE-2	Adjacent side void	1	2799	2862
CFSTE-3	Trilateral void	1	2467	2565
CFSTE-4	Four sides void	1	2089	2204

Comparing the test results of CFSTE-1 and CFSTE-2, it can be seen that when the density loss rate of square steel tube core concrete is the same, whether it is the opposite side void or the adjacent side void, the ultimate bearing capacity of the specimen is the same. Comparing all the

ISSN: 2472-3703 DOI: 10.6911/WSRJ.202305_9(5).0013

void specimens, it can be seen that when the loss rate of the compactness of the core concrete of the square steel tube is the same, the ultimate bearing capacity of the specimen decreases rapidly with the increase of the number of voids, and the bearing capacity decreases by 21.15 % -41.51 %. The main reason is that when the concrete-filled square steel tube column is axially compressed, the gap between the steel tube and the core concrete weakens the bonding force between the steel tube and the concrete, and weakens the effective constraint of the steel tube on the core concrete. At the same time, before the core concrete is gradually crushed, the steel tube is not effectively supported, and the steel tube and the core concrete fail to show good cooperative work and mutual reinforcement performance throughout the compression process.

It can be seen from Fig.10 and Table 2 that the bearing capacity and stiffness of concrete-filled square steel tubular columns (including void defects) calculated by ABAQUS software are higher than the experimental results. The main reasons are as follows: (1) The refined models established in ABAQUS are assumed to be in the elastic-plastic state under the optimal state, and the materials of each component of the model are assumed to be homogeneous in all directions, but the homogeneity cannot be guaranteed in the actual production of concrete-filled square steel tubular columns. (2) In the process of test loading, when the variational table is used to measure the axial displacement of the concrete-filled square steel tubular column, the error of the small gap between the concrete-filled square steel tubular column and the surface of the upper and lower bearing plates of the loading machine cannot be completely eliminated [11-12]; (3) The concrete-filled square steel tubular column model built by ABAQUS is in an ideal state when simulating axial compression. The interaction between the components of the model is fixed contact. However, in the actual axial compression process, the concrete-filled square steel tubular may be disturbed by external uncertainties, which makes the specimen unable to maintain the ideal state.

5. CONCLUSION

Compared with the axial compression test of concrete-filled square steel tubular columns with void defects in the same research group, the accuracy of the axial compression model of concrete-filled square steel tubular columns with void defects established by ABAQUS finite element software is verified. The error of the ultimate bearing capacity and load-displacement curve of the specimen is within 10 %.

2) When the core concrete loss rate is 1 %, the loss of bearing capacity caused by the opposite side void and the adjacent side void is almost the same.

3) When the core concrete loss rate is 1 %, with the increase of the number of voids, the bearing capacity of the specimen decreases rapidly, the descending section of the load-displacement curve is steep, and the deformation capacity of the specimen decreases.

REFERENCES

[1] Dong Yaxing, Tong Sixian, Ren Ning, et al.Research on concrete pouring technology of steel tube column [J].Building technology development, 2018,45 (08) : 31-32.

[2] Chen, Wei, Zhou et al.. Application status and prospect of CFST arch bridge in China [J]. Journal of Civil Engineering, 2017,50 (06) : 50-61

[3] Chen Xing, Luo Chiyu, Wang Hualin, et al. Innovation and Application of Steel-Concrete Hybrid Structures in Tall Buildings [J]. Building Structures, 2020, 50 (10) : 1-11.

[4] Liao F Y, Han L H, Zhong T. Behaviour of CFST stub columns with initial concrete imperfection: Analysis and calculations [J]. Thin-Walled Structures, 2013, 70(sep.): 57-69.

ISSN: 2472-3703 DOI: 10.6911/WSRJ.202305_9(5).0013

[5] Han L H, Ye Y, Liao F Y. Effects of Core Concrete Initial Imperfection on Performance of Eccentrically Loaded CFST Columns [J]. Journal of Structural Engineering, 2016, 142(12): 04016132.

[6] Lu Z, Guo C. Effects of SWS Strength and Concrete Air Void Composite Defects on Performance of CFST Arch Bridge Rib [J]. Mathematical Problems in Engineering, 2020, 2020:1-18.

[7] Guo C, Lu Z. Air Void and Cap Gap Composite Defects of Concrete-Filled Steel-Tube Arch Bridge Transverse Brace [J]. Journal of Performance of Constructed Facilities, 2020, 34(4): 04020073.

[8] Wang J F, Liu W, Shen Q h et al., Experimental investigation and theoretical analysis of axially-loaded concrete-filled elliptical tubes with circumferential gaps. Thin-Walled Structures, 2022. 181: p. 110100.

[9] Introduction guide of ABAQUS finite element software version 6.4 [M]. Beijing : Tsinghua University Press, 2004.

[10] Wang Yu 's Bracelet. ABAQUS Structural Engineering Analysis and Example Explanation [M]. Beijing : China Construction Industry Press, 2010.

[11] Li Bin, Li Xile. Finite element analysis of the influence of axial compression ratio on the mechanical behavior of rectangular concrete-filled steel tubular frame [J].Journal of Inner Mongolia University of Science and Technology, 2007 (03) : 257-260. 2095-2295.

[12] Lu Z H, Zhao Y G. Suggested empirical models for the axial capacity of circular CFT stub columns [J]. Journal of Constructional Steel Research, 2010, 66(6): 850-862.